# A Peculiar Jet and Arc of Molecular Gas Toward the Rich and Young Stellar Cluster Westerlund 2 and a TeV Gamma Ray Source

Yasuo Fukui,[1] Naoko Furukawa,[1] Thomas M. Dame,[2] Joanne R. Dawson,[1,3] Hiroaki Yamamoto,[1] Gavin P. Rowell, [4] Felix Aharonian,[5,6] Werner Hofmann,[6] Emma de Oña Wilhelmi,[6] Tetsuhiro Minamidani,[7] Akiko Kawamura,[1] Norikazu Mizuno,[1, 8] Toshikazu Onishi,[1] Akira Mizuno,[9] Shigehiro Nagataki [10]

[1]*Department of Astrophysics, Nagoya University, Furocho, Chikusa-ku, Nagoya, Aichi, 464-8602*

[2]*Harvard-Smithsonian Center for Astrophysics, 60 Garden Street, Cambridge MA 02138, USA.*

[3]*Australia Telescope National Facility, CSIRO, P.O. Box 76, Epping NSW 1710, Australia*

[4]*School of Chemistry and Physics, University of Adekaide, Adelaide 5005, Australia.*

[5]*Dublin Institute for Advanced Studies, 31 Fitzwilliam Place, Dublin 2, Ireland.*

[6]*Max-Planck-Institut fur Kernphysik, PO Box 103980, 69029 Heidelberg, Germany.*

[7]*Department of Physics, Faculty of Science, Hokkaido University, N10W8, Kita-ku, Sapporo 060-0810*

[8]*National Astronomical Observatory of Japan, Osawa, Mitaka, Tokyo 181-8588, Japan.*

[9]*Solar-Terrestrial Environment Laboratory, Nagoya University, Furocho, Chikusa-ku, Nagoya 464-8601*

[10]*Yukawa Institute for Theoretical Physics, Kyoto University, Sakyo-ku, Kyoto 606-8502*

*fukui@a.phys.nagoya-u.ac.jp*

(Received 2000 December 31; accepted 2001 January 1)

**Abstract**

We have discovered remarkable jet- and arc-like molecular features toward the rich and young stellar cluster Westerlund2. The jet has a length of $\sim 100$ pc and a width of $\sim 10$ pc, while the arc shows a crescent shape with a radius of $\sim 30$ pc. These molecular features each have masses of $\sim 10^4 M_\odot$ and show spatial correlations with the surrounding lower density HI gas. The jet also shows an intriguing positional alignment with the core of the TeV gamma ray source HESS J1023-575 and with the MeV/GeV gamma-ray source recently reported by the *Fermi* collaboration. We argue that the jet and arc are caused by an energetic event in Westerlund 2, presumably due to an anisotropic supernova explosion of one of the most massive member stars. While the origin of the TeV and GeV gamma-ray sources is uncertain, one may speculate that they are related to the same event via relativistic particle acceleration by strong

shock waves produced at the explosion or by remnant objects such as a pulsar wind nebula or microquasar.

**Key words:** ISM: molecules, stars: individual (Westerlund 2), acceleration of particles, stars: supernovae: general

## 1. Introduction

Massive stars have a strong influence on the surrounding interstellar space via their stellar winds and ultraviolet radiation. Moreover, they end their lives in catastrophic supernova (SN) explosions, thus providing more energetic impact on the interstellar medium. Wd2 is a rich star cluster of age $2-3$ Myrs (Piatti et al. 1998). CO observations have allowed a distance estimate to the source of $5.5 \pm 1.5$ kpc (Furukawa et al. 2009; see also Dame 2007). The total stellar mass in Wd2 is of the order of $4500 M_{\odot}$, including 12 O stars and 2 WR stars (Rauw et al. 2007). It is also associated with a HII region RCW49, a remarkable infrared nebula as revealed by *Spitzer* (Churchwell et al. 2004), and perhaps with the extended TeV gamma-ray source HESS J1023-575, discovered with the HESS telescope array in the direction of the cluster (Aharonian et al. 2007). Recently, low energy (MeV/GeV) gamma-rays have been reported from the same direction by the *Fermi* collaboration (Abdo et al. 2009).

In this Letter we describe the discovery of a spectacular jet and arc of molecular gas detected with the NANTEN telescope in the $^{12}$CO($J = 1-0$) mm-wave emission line survey (Mizuno & Fukui 2004), and discuss their possible links to the MeV/GeV and TeV gamma-ray sources.

## 2. Results

We show the two new CO features toward Wd2 in Figure 1, where the CO distribution in the velocity range $\sim 20-30$ km s$^{-1}$ is presented in Galactic coordinates. One is a straight feature in the east at $(l, b) = (284^{\circ}.2 - 284^{\circ}.9, -1^{\circ}.0 - -0^{\circ}.4)$ (hereafter, the jet) and the other an arc-like feature in the west at $(l, b) = (283^{\circ}.9 - 284^{\circ}.3, -0^{\circ}.5 - 0^{\circ}.0)$ (hereafter, the arc). We note that the arc has an intensity peak and a protrusion to the west of HESS J1023-575 at $(l, b) = (284^{\circ}.04 - 284^{\circ}.09, -0^{\circ}.31 - -0^{\circ}.24)$, both of which lie along the jet axis, suggesting the existence of the diametrically opposite part of the jet.

These two features show a remarkable correlation with Wd2 / HESS J1023-575. The jet is extended over $1^{\circ}$ to the east of Wd2 / HESS J1023-575, tilted at an angle of $\sim 39^{\circ}$ to the galactic plane, and is very well aligned with Wd2 / HESS J1023-575 as well as a ridge of the radio continuum corresponding to the HII region, RCW 49(Whiteoak & Uchida 1997). A least-squares fitting to the jet in Figure 1 yields a regression,

$$b + 1^{\circ}.0 = (-2'.50 \pm 0'.20) + (0.81 \pm 0.01)(l - 285^{\circ}.0), \quad (1)$$

where $l$ and $b$ are in degrees.

This line passes through the $1\sigma$ error box of the peak position of HESS J1023-575, which is shifted from the center of the cluster by $\sim 6$ arcmin. The arc is apparently symmetric with respect to the jet axis and is well centered on HESS J1023-575. It appears somewhat rim-brightened along the outer boundary and shows a marked crescent shape, suggesting part of a swept-up shell. For convenience we define an axis $S$, which runs along the direction of the jet and passes through the peak position of HESS J1023-0575, and an axis $T$ which is perpendicular to $S$. Here the origin of both $T$ and $S$ is $(l, b) = (284^\circ.19, -0^\circ.39)$.

The velocity distributions of the two features are shown in two overlaid velocity channel maps (Figure 2a) and in a position-velocity map along $S$ (Figure 2b).

The jet is generally quiescent, having a velocity width of a few km s$^{-1}$ between $S \sim 0^\circ.1 - 0^\circ.6$ but show fairly large widths of 10 km s$^{-1}$ at $S \sim 0^\circ.5$ and $0^\circ.7$, if all the features are assumed to be physically associated. We tentatively divide the molecular gas towards the jet into the following four components;

J1: A narrow component at $S \sim 0^\circ.0 - 0^\circ.6$ located at $\sim 29$ km s$^{-1}$ with a linewidth of 1 $-$ 2 km s$^{-1}$, with little velocity gradient. This component has three local peaks at $S \sim 0^\circ.2, 0^\circ.3$, and $0^\circ.5$ with a winding shape towards $S \sim 0^\circ.1 - 0^\circ.3$.

J2: A broad component at $S \sim 0^\circ.6 - 1^\circ.0$ located over a velocity range of 19 $-$ 30 km s$^{-1}$.

J3: A fairly broad and localized feature at $S \sim 0^\circ.5$ and $V_{\rm LSR} \sim 21 - 24$ km s$^{-1}$, towards one of the peaks of J1.

J4: The western component partially overlapping with the arc at $S \sim -0^\circ.2$ and $V_{\rm LSR} \sim 26$ km s$^{-1}$.

Although it is not conclusive, we suggest that the four components of the jet are physically related as discussed later. The $^{12}$CO linewidth of the arc is $\sim 4$ km s$^{-1}$ centered at 26 km s$^{-1}$, and we infer that the possible expansion velocity of the arc is not large.

We shall here assume that the jet and arc are at $\sim 5.4$ kpc with a 30% error limit, and estimate the mass of each as follows, where an X factor of $2.0 \times 10^{20}$ cm$^{-2}$ (K km s$^{-1}$) is used to convert the $^{12}$CO intensity to molecular mass (Bertsch et al. 1993): $M({\rm J1}) \sim 7.9 \times 10^3 M_\odot$, $M({\rm J2}) \sim 2.2 \times 10^4 M_\odot$, $M({\rm J3}) \sim 3.0 \times 10^3 M_\odot$, $M({\rm J4}) \sim 1.0 \times 10^3 M_\odot$, and $M({\rm arc}) \sim 2.0 \times 10^4 M_\odot$, respectively. The accuracy in mass is limited to $\pm 60\%$ because of the uncertainty in distance.

We show the HI distribution at $V_{\rm LSR} = 25.56$ km s$^{-1}$ with a width of 0.82 km s$^{-1}$ in Figure 3 (McClure-Griffiths et al. 2005). The HI shows a clear sign of a hole towards Wd2 and HESS J1023-575. Hereafter we shall call the HI feature surrounding the hole the HI shell. This shell is seen over a velocity range of 18 $-$ 32 km s$^{-1}$. We note that the velocity width of the hole is rather small, a few km s$^{-1}$, suggesting that the possible expansion velocity is small at present. The HI hole has an elliptical shape with dimensions of $\sim 29$ pc by $\sim 14$ pc, elongated along the direction of S. It is noteworthy that the HI shell exhibits an intensity

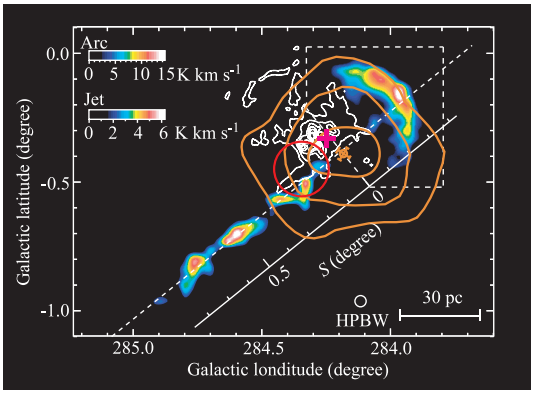


**Fig. 1.** The distribution of the $^{12}$CO emission integrated over a velocity range from $24 - 28$ km s$^{-1}$ (the arc in the dashed region) and from $28 - 30$ km s$^{-1}$ (the jet). The orange contours correspond to the TeV gamma ray source, HESS J1023-575 (Aharonian et al. 2007). The red circle indicates the location of the gravity centre of the low energy (MeV/GeV) gamma-ray source reported by the *Fermi* collaboration (Abdo et al. 2009). The white contours are the radio continuum (Whiteoak & Uchida 1997). The cross indicates the position of Wd2. The axis S is defined along the direction of the jet with the position of HESS J1023-575.

depression in its northern part, coincident with the molecular arc, suggesting that the arc and shell are physically related. This HI intensity depression is likely due to the conversion of HI into $H_2$. The jet is coincident with an elongated spur of HI extended to the east over $\sim 1°$, from $l \sim 284°.3$ to $285°.0$, while on the west there is little HI beyond the arc. The HI mass of the cloud shown in Figure 3 amounts to $\sim 1.5 \times 10^5 M_\odot$ in the velocity range $18 - 32$ km s$^{-1}$ for a conversion factor of $1.8 \times 10^{18}$ cm$^{-2}$ (K km s$^{-1}$)$^{-1}$ (Dickey et al. 1990).

## 3. Discussion

The CO arc and HI shell suggest a spherical shock either due to a SN or stellar winds of WR stars. The secure lower limit for the kinetic energy involved in the arc is estimated to be $\sim 2.0 \times 10^{47}$ ergs for a molecular mass of $\sim 2.0 \times 10^4 M_\odot$ and an expansion velocity of 1 km s$^{-1}$. A more likely estimate is perhaps $\sim 1 \times 10^{48}$ ergs or more if we add the expansion energy of the HI gas to the expansion energy of the gas traced in CO. A SN with mechanical energy $\sim 10^{51}$ ergs is more than sufficient to account for the energetics of the observed molecular and atomic gas, even when taking into account the conversion efficiency into kinetic energy of $\sim 0.1$ (Thornton et al. 1998). There are many O stars in Wd2, whose collective mechanical wind energy may be large. For example 10 O-stars each with stellar-wind kinetic energy luminosities of $10^{36}$ erg s$^{-1}$ yield $\sim 10^{37}$ erg s$^{-1}$. Over a timescale of $\sim 10^5$ years the total kinetic power could reach $\sim 3 \times 10^{49}$ ergs. With the same conversion efficiency, 0.1, a kinetic energy of $\sim 3 \times 10^{48}$ ergs is available.

The one-sided molecular jet can be explained in terms of in-situ conversion of HI into molecular gas by shock compression as a result of the jet propagating through the atomic

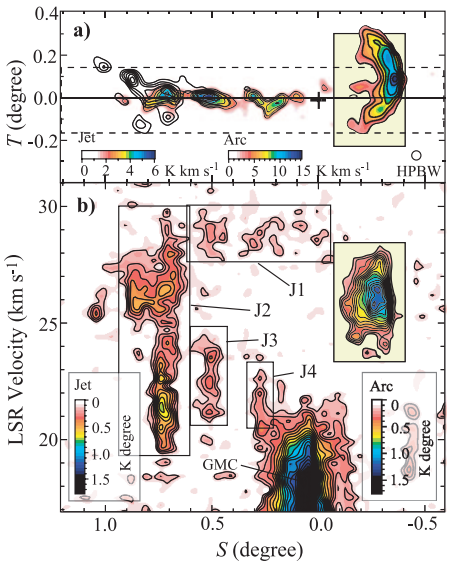


**Fig. 2.** Velocity distribution of the arc and the jet along the axis of the jet. (a) Integrated intensity map in $^{12}$CO emission. The velocity ranges are 24 − 28 km s$^{-1}$ for the arc and 28 − 30 km s$^{-1}$ for the jet. Dashed contours show emission in the range 25 − 28 km s$^{-1}$ and are every 1.6 K km s$^{-1}$ from 2.4 K km s$^{-1}$ ($\sim 3\sigma$). The blue mark indicates the position of the TeV gamma ray source. (b) Position-velocity diagram taken along $S$ in figure 1. The horizontal axis indicates the coordinate of $S$ with the position of the TeV gamma ray source as the origin. The definitions of the components J1, J2 and J3 are described in the text.

medium over a projected length of $\sim 100$ pc. This is consistent with the huge mass of the molecular jet − several times $10^4 M_\odot$ − and the considerable amount of HI gas ($\sim 5.2 \times 10^4 M_\odot$ ) seen towards it. A lower limit for the time scale of the molecular jet is estimated to be $\sim 10^{5-6}$ yrs from the timescale of shocked CO formation (Koyama & Inutsuka 2000; Bergin et al. 2004). There are presently two other known candidates for molecular jets driven by high-energy jets − SS433 and MJG348.5 (Yamamoto et al. 2008). The physical parameters of the two molecular jets are estimated as follows; full length $\sim 500$ pc, molecular mass $\sim 10^4 M_\odot$, and minimum kinetic energy $\sim 10^{48}$ ergs. For the Wd2 clouds, we roughly estimate such kinetic energy to be $\sim 2.0 \times 10^{48}$ ergs from the mass, $\sim 2.2 \times 10^4 M_\odot$, and the velocity span, $\sim 10$ km s$^{-1}$, of the dominant component J2, which is somewhat larger than the above two cases. We note that an increased velocity dispersion at the far tip of the jet, as seen in J2, is also observed in SS433 and MJG348.5. This is interpreted as a result of the stronger dynamical interaction towards the tip of the jet, where the deceleration of the high-energy jet becomes most significant (Yamamoto et al. 2008).

We now consider the origin of the jet and arc. Presently, there are two scenarios in which highly collimated flows of sufficient energy and length may be formed: (i) a highly anisotropic supernova explosion; (ii) a high-energy accretion-powered jet from a compact object such as in a microquasar. Anisotropic energy output is thought to have occurred in several known SNe

including Cas A and W49B (Hwang et al. 2004; Miceli et al. 2008). The expected speed of the jets is $> 1000$ km s$^{-1}$, suggesting a travel time of $\sim 10^4$ yrs over $\sim 100$ pc if the jet axis is nearly perpendicular to the line of sight. Theoretical calculations indicate that a strongly magnetized and rotating neutron star formed in a SNe results in highly collimated jet (Burrows et al. 2007). Such explosions are able to release $> 10^{52}$ ergs in energy (Komissarov & Barkov 2007), and the compact remnant is expected to be observable as a magnetar. The frequency of known magnetars is low, with only 12 magnetars (Mereghetti 2008) amongst the 1500 or so known pulsars (Manchester 2004), while jet-like features in historical SNRs such as Cas A suggest that the anisotropic SNe may not be very rare. To summarize, the anisotropic SNe scenario may well explain the jet and arc as caused by a single collimated SNe.

An alternative is that a conventional, isotropic SNe occurred in a binary system, leading to the formation of an accretion-powered jet. For example, the microquasar SS433, exhibits an X-ray jet of 150 pc and molecular jet of 400 pc in length (Kotani 1998; Yamamoto et al. 2008). In Wd2 the arc and shell might be formed by the SN explosion, and the molecular jet by a long-lived microquasar jet. The SS433 jet has a momentum flow rate of $1.5 \times 10^{-7} M_\odot$ yr$^{-1}$ and can supply $10^{51}$ ergs in kinetic energy in $10^5$ yrs (Kotani 1998; Marshall et al. 2002), sufficiently large to supply the kinetic energy above.

Concerning the origin of the gamma-ray emission, the intriguing alignment of the gravity centers of both the *Fermi* and HESS source positions with the molecular jet and arc suggests a common (initial) event, e.g., a supernova explosion. The link could be direct, via radiation of relic particles produced at the SN explosion, or via on-going acceleration of particles by a relativistic object such as a remnant of the explosion, e.g. supernova remnant shell, a pulsar wind nebula (PWN) or a microquasar jet. The first scenario favors a hadronic origin for the gamma-ray emission. Because of severe radiative (synchrotron and inverse Compton) losses, the relic ultrarelativistic electrons hardly could survive to the present epoch. Indeed, for any reasonable parameters characterizing the ambient medium, the lifetime of multi-TeV electrons is significantly shorter than the age of the system. On the other hand, inverse Compton radiation of gamma-rays by continuously accelerated electrons, e.g., by a PWN, is a viable option. The gamma-ray luminosity is about $10^{35}$ erg s$^{-1}$. If the main target for IC gamma-rays is the 2.7 K CMBR, this mechanism would require acceleration of TeV electrons at a rate of $10^{37}$ erg s$^{-1}$, or an order of magnitude less, if the optical radiation of stars plays a dominant role. The latter case can be realized when acceleration and radiation of electrons take place not far from the stars. The extended character of the gamma-ray emission excludes a single star origin for the observed TeV emission. In this case the extension of the gamma-ray source is effectively determined by the volume occupied by stars, and consequently the size of the source is expected to be energy-independent. In contrast to this scenario, for a single PWN we expect an energy-dependent morphology caused by radiative energy losses which do not allow the highest energy electrons to propagate to large distances. Such an effect is observed in the

PWN HESS J1825-137 (Aharonian et al. 2006). In the case of a hadronic scenario we expect just the opposite dependence. Since generally the higher energy protons propagate faster than low energy protons, we might expect an increase of the angular size of the source with energy (Aharonian 2004). Another test to distinguish between the hadronic and electronic models is the ratio of GeV and TeV gamma-ray fluxes. In the case of the IC mechanism, we expect suppression of low energy gamma-rays and a rather low GeV/TeV ratio. It is expected that future higher quality GeV and TeV data should allow us to conduct detailed a quantitative study of the morphological and spectral characteristics of the radiation in different energy bands, which could lead to definite conclusions. Here we would prefer to limit the discussion by noting that the total energy required to explain the TeV gamma-ray data reported by the HESS collaboration for a source located at a distance of 5 kpc is about $10^{50}(n/1\mathrm{cm}^{-3})^{-1}$ erg. The CO observations indicate a rather low density of gas in the region that coincides with the location of the TeV gamma-ray source (see above), most likely, $n < 1$ cm$^{-3}$. Then the total budget in relativistic protons is required as large as $10^{50}$ erg. This can be considered as an argument in favor of a very strong SN explosion with total energy exceeding $10^{51}$ erg.

In summary, our observations conducted with the NANTEN telescope in the $^{12}$CO($J = 1-0$) mm-wave emission led to the discovery of a spectacular jet and arc of molecular gas toward the young star cluster Westerlund 2 which may be the result of a powerful supernova explosion. Another consequence of this explosion could be the GeV and TeV gamma-ray sources located in the same region as reported recently by the *Fermi* and HESS collaborations. Further detailed studies of spectral and morphological features of gamma-ray emission are requited to explore the links between these two phenomena.

The original NANTEN telescope was operated based on a mutual agreement between Nagoya University and the Carnegie Institution of Washington. This work is financially supported in part by a Grant-in-Aid for Scientific Research (KAKENHI) from the MEXT and from JSPS, in part, through the core-to-core program and by the donation from individuals and private companies.

## References

Abdo, A. A. et al. 2009, submitted.

Aharonian, F. et al. 2004, Very high energy cosmic gamma radiation : A crucial window on the extreme Universe (River Edge, NJ: World Scientice Publishing), Chapter 4

Aharonian, F. et al. 2006, A&A, 460, 365

Aharonian, F. et al. 2007, A&A, 467, 1075

Bergin, E. A., Hartmann, L. W., Raymond, J. C., & Ballesteros-Paredes, J., 2004, ApJ, 612, 921

Bertsch, D. L., Dame, T. M., Fichtel, C. E., Hunter, S. D., Sreekumar, P., Stacy, J. G., & Thaddeus, P. 1993, ApJ, 416, 587

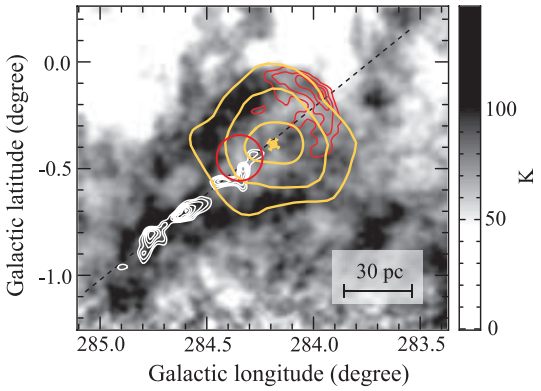


**Fig. 3.** Intensities of the HI and $^{12}$CO emission at a velocity of 25.56 km s$^{-1}$ (McClure-Griffiths et al. 2005). The gray scale is HI emission with an intensity range of 0-150 K. Red and white contours show the integrated intensity of the arc and the jet. The yellow contours correspond to the TeV gamma ray source. The red circle shows the gravity center of the *Fermi* source.


Burrows, A., Dessart, L., Livne, E., Ott, C. D., & Murphy, J. 2007, ApJ, 664, 416

Churchwell, E. et al. 2004, ApJS, 467, 1075

Dame, T. M. 2007, ApJ, 665, 163

Dickey, J. M., Lockman, F. J. 1990, A&A Rev., 28, 215

Furukawa, N. et al. 2009, submitted.

Hwang et al. 2004, ApJ, 615, 117

Komissarov, S. S., & Barkov, M. V. 2007, MNRAS, 382, 1029

Kotani, T. 1998, Doctoral Thesis of University of Tokyo

Koyama, H., & Inutsuka, S. 2000, ApJ, 532, 980

Manchester, R. N. 2004, science, 304, 542

Marshall, H. L., Canizares, C. R., & Schulz, N. S. 2002, ApJ, 564, 941

McClure-Griffiths, N. M., Dickey, J. M., Gaensler, B. M., Green, A. J., Haverkorn, M., & Strasser, S. 2005, ApJS, 158, 178

Mereghetti, S. 2008, A&A Rev.15, 225

Miceli, M., Decourchelle, A., Ballet, J., Bocchino, F., Hughes, J., Hwang, U., & Petre, R. 2008, Adv. Space Research, 41, 390

Mizuno, A., & Fukui, Y. 2004, in ASP Conf. Ser., 317, Milky Way Surveys: The Structure and Evolution of our Galaxy, ed. D. Clemens, R. Y. Shah, & T. Brainerd, 59

Piatti, A. E., Bica, E., & Claria, J. J. 1998, A&AS, 127, 423

Rauw, G., Manfroid, J., Gosset, E., Naze, Y., Sana, H., De Becker, M., Foellmi, C., & Moffat, A. F. J. 2007, A&A, 463, 981

Thornton, K., Gaudilitz, M., Janka, H.-Th., & Steinmetz, M. 1998, ApJ, 500, 95

Whiteoak, J. B. Z., & Uchida, K. I. 1997 A&A, 317, 563

Yamamoto, H. et al. 2008 PASJ, 60, 715